Indeed, in certain instances the less active enantiomer may even possess undesirable properties.[20] Thus, enantiomeric purity is an important criterion for establishing the pharmaceutical acceptability of such drugs.

Acknowledgment. This work was supported in part by the National Science Foundation (B.L.K.). L.R.G. gratefully acknowledges the support of a United States Pharmacopeia Fellowship and the Food and Drug Administration Science Advisor Research Associate Program. The authors thank M. J. Cohen for analysis of the stationary phases and H. Maksoud for mass spectral analysis.

Registry No. I, 92984-07-1; II, 92984-08-2; IV, 67492-08-4; *dl*-phenylethanolamine, 1936-63-6; (*R*)-phenylethanolamine, 2549-14-6; (*S*)-phenylethanolamine, 56613-81-1; *dl*-phenylpropanolamine, 14838-15-4; 1(*R*),2(*S*)-(-)-phenylpropanolamine, 492-41-1; 1(*S*),2(*R*)-(+)-phenylpropanolamine, 37577-28-9; *dl*-pseudophenylpropanolamine, 54680-46-5; 1(*R*),2(*R*)-(-)-pseudophenylpropanolamine, 37577-07-4; 1(*S*),2(*S*)-(+)-pseudophenylpropanolamine, 492-39-7; *dl*-norepinephrine, 138-65-8; (*R*)-(-)-norepinephrine, 51-41-2; (*S*)-(+)-norepinephrine, 149-95-1; *dl*-nordefrin, 74812-63-8; 1(*R*),2(*S*)-(-)-nordefrin, 829-74-3; 1(*S*),2(*R*)-(+)-nordefrin, 829-75-4; *dl*-normetanephrine, 709-52-4; (*R*)-normetanephrine, 2282-53-3; (*S*)-normetanephrine, 35778-41-7; *dl*-1-amino-2-propanol, 1674-56-2; (*R*)-(-)-1-amino-2-propanol, 2799-16-8; (*S*)-(+)-1-amino-2-propanol, 2799-17-9; *dl*-valinol, 16369-05-4; (*R*)-(-)-valinol, 4276-09-9; (*S*)-(-)-valinol, 2026-48-4; *dl*-alaninol, 6168-72-5; L-proline, 2812-46-6; ω-undecenal, 112-45-8; dimethylchlorosilane, 1066-35-9; copper, 7440-50-8.

(20) (a) Weiner, N. "Pharmacological Basis of Therapeutics", 6th ed.; Gilman, A. G.; Goodman, L.; Gilman, A., Ed.; Macmillan: New York, 1980; pp 138-175. (b) Tye, A.; Baldesberger, R.; LaPidus, J. B.; Patil, P. N. *J. Pharmacol. Exp. Ther.* **1967**, *157*, 356-362. (c) Patil, P. N.; Jacobowitz, D. *J. Pharmacol. Exp. Ther.* **1968**, *161*, 279-295. (d) Portoghese, P. A. *Annu. Rev. Pharmacol.* **1970**, *10*, 51-76. (e) Strittmatter, W. J.; Davis, J. N.; Lefkowitz, R. J. *J. Biol. Chem.* **1977**, *252*, 5472-5477. (f) Bukowiecki, L.; Follea, N.; Paradis, A.; Collet, A. *Am. J. Physiol.* **1980**, *238*, E552-E563. (g) Arch, J. R. S.; Ainsworth, A. T.; Cawthorne, M. A. *Life Sci.* **1982**, *30*, 1817-1826.

(21) Smith, H. E.; Burrows, E. P.; Miano, J. D.; Mount, C. D.; Sanders-Bush, E.; Solser, F. *J. Med. Chem.* **1974**, *17*, 416-421.

Photoelectron Spectroscopy of the Allylic Anion

John M. Oakes and G. Barney Ellison*

Contribution from the Department of Chemistry, Campus Box 215, University of Colorado, Boulder, Colorado 80309. *Received June 8, 1984*

Abstract: We have examined the photodetachment spectra of the allylic anion ($CH_2CHCH_2^-$) and two of its deuterated isotopes, $CH_2CDCH_2^-$ and $CD_2CDCD_2^-$. The electron affinities (EA) of the corresponding allyl radicals are EA(CH_2CHCH_2) = 0.362 ± 0.020 eV, EA(CH_2CDCH_2) = 0.373 ± 0.020 eV, and EA(CD_2CDCD_2) = 0.381 ± 0.026 eV. The photoelectron spectra of these ions show only one active vibronic mode which we assign as the in-plane C-C-C bend. This leads us to conclude that the anion has a planar, symmetric C_{2v} geometry. Computational modeling yields a geometry for the $CH_2CHCH_2^-$ ion with a C-C-C bond angle 16° greater than that of the allyl radical.

Almost since radicals have been known to exist, the allyl radical ($CH_2CH{=}CH_2$) has been of fundamental interest to chemists because it is the simplest of conjugated hydrocarbon radicals. For this reason much work has been done to study its thermochemistry and spectroscopy, in addition to a great deal of theoretical effort directed at understanding its electronic structure. The geometry of the allyl radical is qualitatively understood from electron spin resonance (ESR) studies[1-3] and matrix infrared absorption spectra of this important hydrocarbon. All experimental and theoretical studies of allyl radical find it to be a planar molecule with C_{2v} symmetry. A detailed computational study of its geometry and vibrational spectrum has been published recently.[4] The electron affinity has been reported[5] for the allyl radical in an ion cyclotron resonance (ICR) threshold photodetachment experiment, but this is in slight disagreement with flowing afterglow results.[6-8]

The corresponding anion ($CH_2{=}CHCH_2^-$) has also generated much study. Of fundamental interest is the question of whether the geometry of the allylic anion still has C_{2v} symmetry. Earlier studies[9] have focused on a related simple organic radical which is a flat, symmetric, resonance stabilized molecule, the propargyl radical ($CH_2{-}C{\equiv}CH$). It is found that the corresponding ion, $CH{=}_2C{=}CH^-$, is a nonplanar molecule and not conjugatively stabilized. Rather little is known about the structure of the allylic anion. There is some chemical evidence that the two ends of the negative ion behave similarly in the gas-phase experiments.[10] This would lead one to suspect it still has a symmetric, C_{2v} structure. Theoretical structural studies have predicted both planar and nonplanar structures. A multiphoton infrared photodetachment study has recently been made of this ion as well.[11]

Using negative ion photoelectron spectroscopy,[12,13] we have studied the allylic anion (m/z 41) using both propene and 1,5-hexadiene as ion precursors. We have also studied two deuterium-substituted isomers, $CH_2CDCH_2^-$ (m/z 42) and $CD_2CDCD_2^-$ (m/z 46), from the corresponding propenes. From the appearance of the photoelectron spectrum of the allylic ion and by comparison to those of the two deuterated isomers, we conclude that the allylic anion retains its planar, C_{2v} structure. The major structural change observed is the opening of the skeletal C-C-C bond angle. Our analysis quantifies this geometry change and also yields a refined electron affinity of $CH_2{=}CH{-}CH_2$.

Experimental Section

The negative ion photoelectron spectrum is obtained by intersecting a mass-selected ion beam with a laser of fixed frequency ($\hbar\omega_0$) and determining the distribution of kinetic energy (KE) for the detached electrons $M^- + \hbar\omega_0 \rightarrow M + e^-$ (KE). Although the photoelectron

(1) J. K. Kochi and P. K. Krusic, *J. Am. Chem. Soc.* **90**, 7158 (1968).
(2) R. W. Fessenden and R. H. Schuler, *J. Chem. Phys.*, **39**, 2147 (1963).
(3) J. K. Kochi, *Adv. Free-Radical Chem.*, **5**, 224 (1975).
(4) T. Takada and M. Dupuis, *J. Am. Chem. Soc.*, **105**, 1713 (1983).
(5) A. H. Zimmerman and J. I. Brauman, *J. Am. Chem. Soc.*, **99**, 3565 (1977).
(6) V. M. Bierbaum, R. J. Schmitt, and C. H. DePuy, Environment. Health Perspect., **36**, 119 (1980).
(7) G. I. McKay, M. H. Lien, A. C. Hopkinson, and D. K. Bohme, *Can. J. Chem.*, **56**, 131 (1978).
(8) D. K. Bohme and L. B. Young, *J. Am. Chem. Soc.*, **92**, 3301 (1970).
(9) J. M. Oakes and G. B. Ellison, *J. Am. Chem. Chem. Soc.*, **105**, 2969 (1983).
(10) G. Klass, V. C. Trenerry, J. C. Sheldon, and J. H. Bowie, *Aust. J. Chem.*, **34**, 518 (1981).
(11) C. H. Wight and J. L. Beauchamp, *J. Phys. Chem.*, **88**, 4426 (1984).
(12) W. C. Lineberger In "Chemical and Biochemical Application of Lasers", Vol. 1, C. B. Moore, Ed., John Wiley, New York, 1974, Chapter 5, pp 139-162.
(13) B. K. Janousek and J. I. Brauman In "Gas Phase Ion Chemistry", Vol. 2, M. Bowers, Ed., Academic Press, New York, 1979, Chapter 10, pp 53-86.

0002-7863/84/1506-7734$01.50/0

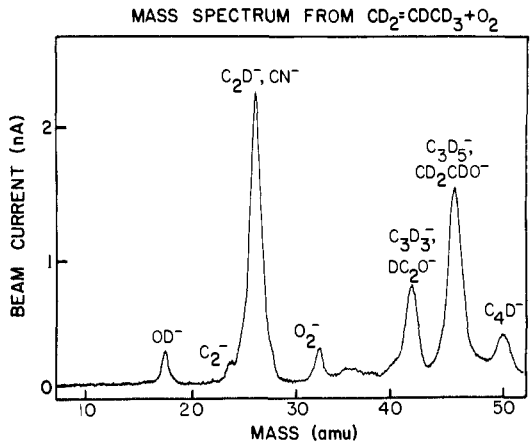

Figure 1. Negative ion mass spectrum resulting from a mixture of CD_2=CD—CD_3/O_2.

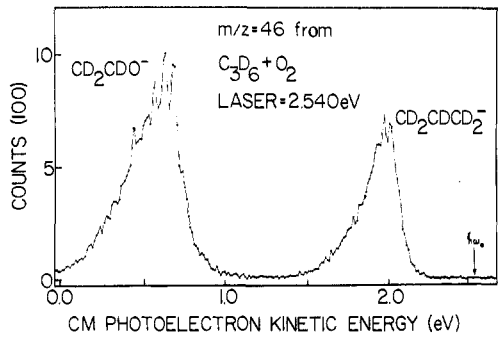

Figure 2. A survey photoelectron spectrum of the $C_3D_5^-$ ion (roughly 11 meV between data points). The center of mass (CM) photoelectron kinetic energy of the scattered electrons is plotted against the total number of electron counts.

spectrometer used in this experiment has been described in detail previously,[14] we will briefly outline our procedure. A beam of negative ions is extracted from a high-pressure discharge ion source which contains the ion precursor(s). The beam is dispersed according to mass by a Wien filter before entering a high-vacuum region (10^{-9} torr). This mass-selected beam ($\simeq$1 nA) is intersected at 90° by a fixed frequency (4880 Å, 75 W) beam from an argon ion laser. Those electrons scattered at right angles to both the ion and the laser beams enter our double hemispherical electron energy analyzer. The resolution of this analyzer (fwhm) is roughly 20 meV.

The allylic anion is produced in our ion source with use of a tungsten filament by adding either approximately a 1:1 mixture of propylene (Matheson Gas Products) and O_2 or neat 1,5-hexadiene (Aldrich) to our ion source. The deuterated allyl ions were produced from a 1:1 mixture of either propene-2-d_1 (CH_3—CD=CH_2) or perdeuteriopropylene plus O_2. Both propenes were obtained from Merck, Sharpe and Dohme. Their purity (99%) was confirmed by infrared spectroscopy, and the compounds were used without further purification.

It is important to discuss the manner in which we identified the allylic ions. Approximately 200 pA of $C_3H_5^-$ was obtained from neat 1,5-hexadiene. The mass of the ion we believe to be allylic (m/z 41) was confirmed by detaching the ion of m/z 39 near it in the spectrum. This ion is the allenyl anion ($C_3H_3^-$) which has been studied previously.[9]

From propylene/O_2 we obtain about 1.5 nA of the m/z 41 ion. This proves to consist of roughly a 1:1 mixture of $HCCO^-$ and $C_3H_5^-$. Identifying the mass is straightforward because the spectrum[15] of $HCCO^-$ has been reported previously. From propene-2-d_1 and O_2 we obtain a 1-nA beam of an ion with m/z 42. We assign this as $CH_2CDCH_2^-$ and confirm the mass identity by detachment of neighboring ions with m/z 41 ($HCCO^-$) and m/z 44 (CH_2CDO^-). The photoelectron spectrum of CH_2CHO^- has been reported,[16] and the monodeuterated isomer has a similar spectrum.

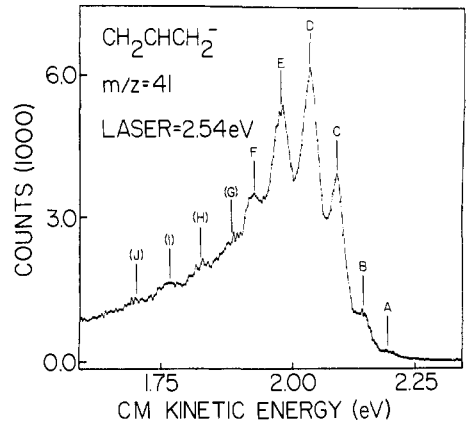

Figure 3. A higher signal-to-noise photoelectron spectrum of the d_0 allylic ion; the data points are roughly 2.8 meV apart.

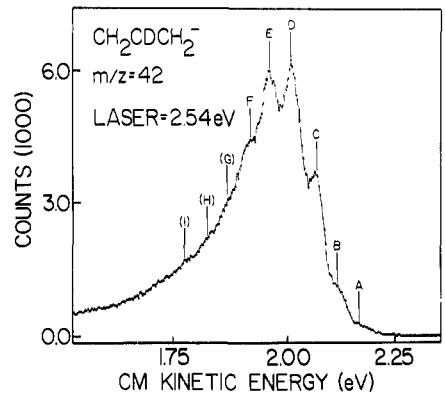

Figure 4. A higher signal-to-noise photoelectron spectrum of the d_1 allylic ion; the data points are roughly 2.8 meV apart.

Figure 1 is the mass spectrum of ions resulting from a mixture of O_2 and perdeuteriopropene. Several of the ions are absolutely identified by their photodetachment spectra (OD^-, O_2^-, $C_3D_3^-$, and DC_2O^-). The ions at m/z 46 are positively assigned as CD_2CDO^- and $C_3D_5^-$. The perdeuteriovinyloxy anion (CD_2CDO^-) has been studied earlier[16] so that the assignment of our mass peak as m/z 46 is secure. Figure 2 is a low-resolution photoelectron spectrum resulting from detachment of the m/z 46 ion beam. The spectrum shows a set of features at low electron energy due to detachment[16] of CD_2CDO^- [EA(CD_2CDO) = 1.819 eV]. Electrons are also seen at relatively high energy which we assign as arising from another m/z 46 ion, $C_3D_5^-$.

All photoelectron spectra we report are calibrated with a reference ion (generally OH^- or OD^-). The spectra are transformed to a center-of-mass (CM) frame by the following relationship.

$$KE = KE_{cal} + \gamma(V - V_{cal}) + mW[(1/M_{cal}) - (1/M)] \quad (1)$$

Here KE is the CM kinetic energy at the point in the spectrum desired, W is the ion beam energy, and m is the mass of the electron. KE_{cal} refers to the kinetic energy of the calibration ion (2.540 − E_{cal}). We have used OH^- and OD^- as our marker ions; the EA of the hydroxyl radical is well-known.[17] V and V_{cal} are the energy analyzer acceleration voltages at the peak in the spectrum, and M and M_{cal} are the masses of the ion being studied and the calibration ion, respectively. An energy scale compresion factor is γ; this factor is determined from the photoelectron spectrum[18] of Cr^- and is typically in the range 1.00 ± 0.01.

Results

Photodetachment spectra of $CH_2CHCH_2^-$, $CH_2CDCH_2^-$, and $CD_2CDCD_2^-$ are presented in Figures 2–6. Figure 2 is a survey spectrum of $C_3D_5^-$ (roughly 11 meV between data points). Besides identifying the mass of the ion, this trace indicates that we are only able to access the ground $\tilde{X}$ state of the radical; our laser

(14) H. B. Ellis and G. B. Ellison, *J. Chem. Phys.*, **78**, 6541 (1983).
(15) J. M. Oakes, M. Jones, V. M. Bierbaum, and G. B. Ellison, *J. Phys. Chem.*, **87**, 4810 (1983).
(16) G. B. Ellison, P. C. Engelking, and W. C. Lineberger, *J. Phys. Chem.*, **86**, 4873 (1982).
(17) P. A. Schulz, R. D. Mead, P. L. Jones, and W. C. Lineberger, *J. Chem. Phys.*, **77**, 1153 (1982).
(18) C. S. Feigerle, R. R. Corderman, S. V. Bobashev, and W. C. Lineberger, *J. Chem. Phys.*, **74**, 1580 (1981).

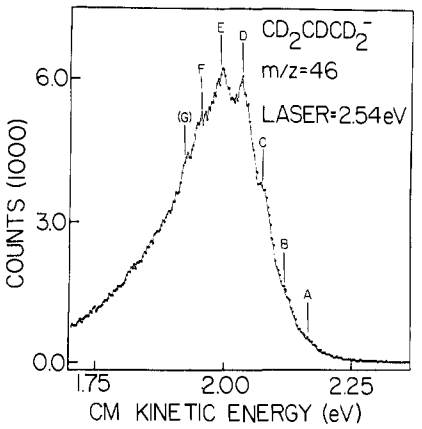

Figure 5. A higher signal-to-noise photoelectron spectrum of the d_5 allylic ion; the data points are roughly 2.8 meV apart.

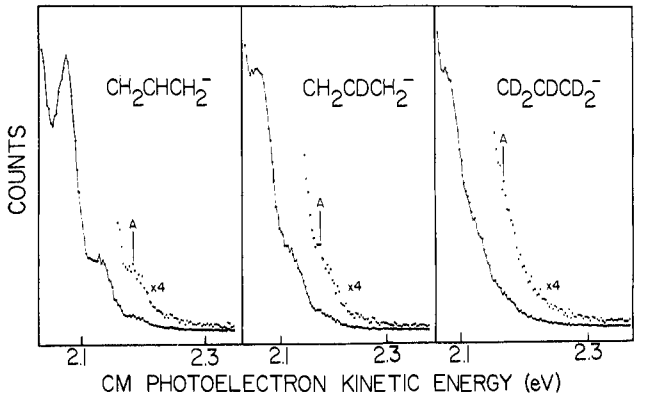

Figure 6. Enhanced plots of the photodetachment origins for the three isotopic allylic ions; the data points are approximately 2.8 meV apart.

is not energetic enough to reach the CD_2CDCD_2 $\tilde{A}$ state. Figures 3–6 are high signal-to-noise spectra (about 2.8 meV between points) which display the features in the spectra more clearly. Figure 6 is a trace through the detachment origin of each of the isomeric ions. In all cases the photoelectron spectrum is a plot of the CM kinetic energy of the electrons detached vs. the number of electrons counted. Electron energy increases to the right, with the highest possible energy being that of the laser photons, $\hbar\omega_0$ = 2.540 eV.

Each of the spectroscopic features in Figures 3–6 are labeled; Table I collects together data from all isomeric ions. The errors quoted in the table are absolute and include contributions from all experimental parameters. Splittings between the peaks will have smaller uncertainties than Table I would indicate (typically 2–4 meV) since many of the factors contributing to the total error bars (such as drifts in ion beam voltage, shifts in γ, and the like) are likely to cancel when differences are computed.

Each of the more detailed spectra (Figures 3–5) shows detachment of the ion to only a single electronic state of allyl radical. From the long Franck–Condon profiles, we deduce that there is a significant geometry difference between the allylic anion and the allyl radical. We will return to this question in a later section of the paper.

The first feature marked in Figures 3–5 is peak A which we believe to be the origin of each of the spectra. Figure 6 depicts this region of the spectrum with a scale enhancement of a factor of 4. Peak A is a prominent in $CH_2CHCH_2^-$ and $CH_2CDCH_2^-$ but is poorly evident in the d_5 ion, $CD_2CDCD_2^-$. This region of the photoelectron spectrum of the allylic ion always appears the same in each of the numerous scans we have taken. It is invariant to ion source conditions, type of filament, or ion precursor. We do not think that peak A results from detachment of a vibrationally excited ion ("hot bands"). Hot band features generally express themselves by different frequency intervals and irregular intensities (see ref 14 for a clear example). The constancy of peak A as well as the regularity of the vibrational progression over the Franck–Condon envelopes in Figures 3–5 leads us to assign the A features as the (0,0) transitions. The difference between the photon energy ($\hbar\omega_0$ = 2.540 eV) and CM kinetic energy is the binding energy; the binding energy of the (0,0) band is the experimental electron affinity. From the values tabulated in Table I, the uncorrected electron affinities are $EA(CH_2CHCH_2)$ = 0.362 ± 0.019 eV, $EA(CH_2CDCH_2)$ = 0.373 ± 0.019 eV, and $EA(CD_2CDCD_2)$ = 0.381 ± 0.025 eV.

Table I. Measured CM Kinetic Energy (eV) of Allylic Ions
Laser λ_0 = 488 nm

peak	CH_2=CH—CH_2^-	CH_2=CD—CH_2^-	CD_2=CD—CD_2^-
A	2.178 ± 0.019	2.167 ± 0.019	2.159 ± 0.025
B	2.129 ± 0.014	2.114 ± 0.014	2.112 ± 0.017
C	2.074 ± 0.010	2.066 ± 0.011	2.068 ± 0.012
D	2.031 ± 0.009	2.005 ± 0.009	2.011 ± 0.009
E	1.982 ± 0.009	1.959 ± 0.011	1.969 ± 0.011
F	1.931 ± 0.011	1.916 ± 0.014	1.927 ± 0.016
G	1.885 ± 0.019	1.873 ± 0.016	1.897 ± 0.016
H	1.833 ± 0.019	1.825 ± 0.018	
I	1.783 ± 0.021	1.776 ± 0.024	
J	1.726 ± 0.021		

Discussion

A. Thermochemistry. To help support our conclusion that peak A is indeed the first in a vibrational progression in the allyl radical, we must compare the EA resulting from this conclusion (0.362 ± 0.019 eV) to the results of other experiments. Zimmerman and Brauman[5] have reported the electron affinity of allyl radical in an ICR threshold photodetachment experiment to be 0.550 ± 0.054 eV. Both of our peaks A and B lie outside of this range and peak C is just barely within it; the ICR number falls between peaks E and D in Figure 3. In determining the EA, however, the ICR detachment cross section was extrapolated by modeling the threshold behavior. It was necessary to do this since a tunable light source of long enough wavelength to directly probe the origin was not available.

On the other hand, ion chemistry studies in a flowing afterglow device have shown[6,8] that the charge-transfer reaction

$$CH_2{=}CHCH_2^- + O_2 \rightarrow O_2^- + CH_2{=}CHCH_2 \quad (2)$$

proceeds rapidly, indicating that $EA(O_2) > EA(allyl)$. The electron affinity of O_2 is well-known[19] to be 0.440 ± 0.008 eV; this implies a bound of $0.0 < EA(CH_2CHCH_2) < 0.440$ eV.

In separate flowing afterglow experiments,[7] the reactions of propene and hydroxide ion were scrutinized to ascertain the gas-phase acidity ($\Delta H°_{acid}$) of the alkene.

$$CH_2{=}CH{-}CH_3 + OH^- = CH_2CHCH_2^- + H_2O \quad (3)$$

MacKay et al.[7] have measured the equilibrium constant for (3); from K_{equi} and the known[20] $\Delta H°_{acid}$(HO–H), they deduce that $\Delta H°_{acid}(CH_2CHCH_2\text{–H})$ = 391.3 ± 0.5 kcal/mol. The gas-phase acidity is simply related to the homolytic bond dissociation energy (DH), EA, and the ionization potential of H [IP(H) = 313.605 kcal/mol].

$$\Delta H°_{acid}(CH_2CHCH_2\text{–H}) = DH°(CH_2CHCH_2\text{–H}) + IP(H) - EA(CH_2CHCH_2) \quad (4)$$

Photoionization mass spectroscopy has provided a value for $DH°(CH_2CHCH_2\text{–H})$. The mass spectrometric appearance potential of $CH_2CHCH_2^+$ from propene has been found[21] to be AP = 11.880 ± 0.030 eV.

$$CH_2{=}CH{-}CH_3 + \hbar\omega \rightarrow CH_2CHCH_2^+ + H + e^- \quad (5)$$

The photoelectron spectrum[22] of the allyl radical shows the IP-

(19) R. J. Celotta, R. A. Bennett, J. L. Hall, M. W. Siegel, and J. Levine, *Phys. Rev. A*, **6**, 631 (1972).
(20) J. E. Bartmess and R. T. McIver In "Gas Phase Ion Chemistry", Vol. 1, M. T. Bowers, Ed., Academic Press, New York, 1979, Chapter 11, pp 87–121.
(21) V. R. Krässig, D. Reinke, and H. Baumgärtel, *Ber. Bunsenges. Phys. Chem.*, **78**, 425 (1974).

Table II. Final Experimental Values

$EA(CH_2CHCH_2) = 0.362 \pm 0.020$ eV
$EA(CH_2CDCH_2) = 0.373 \pm 0.020$ eV
$EA(CD_2CDCD_2) = 0.381 \pm 0.026$ eV
$\Delta H_f°_{298}(CH_2CHCH_2^-) = 29.5 \pm 0.9$ kcal/mol

$(CH_2CHCH_2) = 8.13 \pm 0.02$ eV. The appearance potential, IP, and DH are all related as follows.

$$AP(CH_2CHCH_2^+) = DH°(CH_2CHCH_2\text{–}H) + IP(CH_2CHCH_2) \quad (6)$$

Thus the bond dissociation of propene, $DH°(CH_2CHCH_2\text{–}H)$, is found to be 86.5 ± 0.8 kcal/mol. With use of relationship 4, this suggests a value for $EA(CH_2CHCH_2)$ of 8.8 ± 0.9 kcal/mol [or 0.38 ± 0.04 eV]. This number is significantly smaller than the ICR photodetachment result but is consistent with our assignment of the A peak as the origin.

There are some corrections to be made to our raw electron affinity of 0.362 eV for CH_2CHCH_2. We know little about the rotational constants or vibrational frequencies of CH_2CHCH_2 or $CH_2CHCH_2^-$; consequently, we can only estimate spin–orbit and rotational corrections to our error bars. We adopt a rotational correction of ±0.005 eV as well as a spin–orbit contribution of ±0.001 eV to our final error bars. Since we can assign no hot bands, there is no vibrational sequence band correction[23] to apply. The final value for the $EA(CH_2CHCH_2)$ derived from peak A is 0.362 ± 0.020 eV. Using this value of the EA, we can also compute the $\Delta H_f°_{298}$ of the allylic ion. From the $DH°(CH_2CHCH_2\text{–}H)$ we know that $\Delta H_f°_{298}(CH_2CHCH_2)$ is 39.3 ± 0.8 kcal/mol. The ion heat of formation is obtained[24] from the EA as follows:

$$\Delta H_f°_{298}(CH_2CHCH_2) - \Delta H_f°_{298}(CH_2CHCH_2^-) = EA(CH_2CHCH_2) + 5/2RT \quad (7)$$

In (7) $5/2RT$ is the integrated heat capacity of the electron, 1.481 kcal/mol, consistent with the JANAF convention.[24] We find $\Delta H_f°_{298}(CH_2CHCH_2^-)$ to be 29.5 ± 0.9 kcal/mol. Table II collects our final experimental values for the electron affinities and heats of formation of allyl radicals and the allylic ion.

B. Vibrational Analysis. The structure displayed in the spectra shown in Figures 3–5 belongs to allyl radical and not $CH_2CH\text{-}CH_2^-$. Each of the individual peaks represents detachment of the allylic anion to a different vibrational state of the ground $\tilde{X}\ ^2A_2$ state of CH_2CHCH_2. The molecular spectroscopy of allyl radical has not yet been exhaustively studied. Currie and Ramsay[25] have studied the UV absorption spectrum of the allyl radical produced in flash photolysis of allyl bromide. In this experiment, the $\tilde{A}\ ^2B_1 \leftarrow \tilde{X}\ ^2A_2$ ($T_e = 3.04$ eV) transition was studied. Four vibronic modes in the excited state were observed but not assigned. All the lines were broadened due to predissociation. Little was learned about the vibrational spectroscopy of the ground state of allyl radical.

More recently, Maier et al.[26] have used infrared spectroscopy of matrix-isolated allyl radical from flash pyrolysis using several precursors. All the allowed infrared transitions were observed and assigned. These experimental results are collected in Table III. Of interest is the low-frequency modes seen in the infrared spectrum of allyl.

ESR studies of matrix-isolated CH_2CHCH_2 yield spectra[1-3] consisting of 18 lines, consistent with a C_{2v} radical structure having 3 distinct H atoms in a 1:2:2 ratio. A number of ab initio electronic structure calculations[4,27,28] all find the allyl radical to be a flat, planar species with C_{2v} symmetry. Takada and Dupuis[4] have carried out a careful multiconfigurational Hartree–Fock (MCHF) calculation on CH_2CHCH_2 and then extracted a complete set of harmonic force constants for the $\tilde{X}$ state. These harmonic constants then yield a set of vibrational frequencies for the radicals (Takada and Dupuis consider 3 different isotopically substituted species). We have collected their calculated frequencies in Table III where they are labeled by symmetry and local mode. Although these frequencies may be in error by 10 to 15%, the calculated values in Table III should be a reasonable guide in assigning the vibrational modes of allyl. The calculated frequencies for the deuterated isomers will be a useful guide in assigning the mode we see excited in photodetachment of the selectively isotopically substituted allyl anions.

A qualitative examination of the high-resolution spectrum for $CH_2CHCH_2^-$ in Figure 3 suggests that only one vibrational mode of allyl radical (out of 18 possible) is excited upon detachment of the ion. This mode has a low frequency of about 400 cm^{-1}. A glance at Table III suggests only 3 possible assignments: ω_7, the CCC bend; ω_9, the CH_2 asymmetric twist combination; and ω_{12}, the CH_2 symmetric twist combination. The asymmetric twist was not assigned in the experimental IR studies, while the symmetric twist and the CCC bend were identified. As we will shortly see, the active vibration is the CCC bending mode, ω_7.

We have carried out a least-sqaures fitting analysis to the peak positions tabulated in Table I. Rather than fit the CM kinetic energy for each of the features (A–J), we have fit to the peak binding energies (BE). The BE for a peak is related to the CM kinetic energy through the laser energy, $\hbar\omega_0 = 2.540$ eV. If we subtract the CM kinetic energy from the laser frequency, we recover an experimental BE. These values are collected together in Table IV. We initially fit the BE values to a function of the form:[29]

$$E(v') = T_0 + \omega_7'(v' + \tfrac{1}{2}) + x_{77}'(v' + \tfrac{1}{2})^2 \quad (8)$$

If we fit the experimental BE values to a function of the form of (8), we find excellent agreement. It turns out that the anharmonicity constant for eq 8 which fits our data is on the order of $x_{77}' = 0.0019$ eV or less for all isotopic ions. This is smaller than the experimental peak uncertainties; consequently, we have ignored anharmonicity constants in our energy expression ($x_{77}' \equiv 0$). The final funcations for CH_2CHCH_2, CH_2CDCH_2, and CD_2CDCD_2 are listed in Table IV; we also tabulate the calculated $E(v')$, the difference between the experimental BE and $E(v')$, and the experimental splitting between the various transitions (in cm^{-1}). A glance at the column of differences shows that our fitted, harmonic functions [$E(v')$] match the experimental data to within 10 meV or better in all cases but one.

On the basis of the data of Table IV and the calculated frequencies in Table III, we can assign the active mode in our photoelectron spectra. Of the three low-frequency modes possible, ω_7 most nearly matches our fitted constants: $\omega'(CH_2CHCH_2^-) = 398$ cm^{-1}, $\omega'(CH_2CDCH_2^-) = 391$ cm^{-1}, $\omega'(CD_2CDCD_2^-) = 360$ cm^{-1}. From Table III one can see the extent of the isotope shifts for each isomer. The crucial ratios for us to consider are the following: ω_7 $(CH_2CHCH_2/CD_2CDCD_2) = 0.82$; ω_9 $(CH_2CHCH_2/CD_2CDCD_2) = 0.71$; ω_{12} $(CH_2CHCH_2/CD_2CDCD_2) = 0.77$. The experimentally observed shift is 0.90 (360 cm^{-1}/398 cm^{-1}); this is closest to the value for ω_7. Strictly speaking we should contrast the calculated values in Table III with the (1,0) or fundamental frequencies in Table IV. This is a demanding comparison to make; the first discernible peak (A) in Figures 3–5 is rather weak and difficult to locate precisely. With the proper concern for uncertainties, the fundamental intervals are the following: (0,1) $CH_2CHCH_2 = 395 \pm 165$ cm^{-1}; (0,1)

(22) F. A. Houle and J. L. Beauchamp, *J. Am. Chem. Soc.*, **100**, 3290 (1978).
(23) P. C. Engelking and W. C. Lineberger, *J. Chem. Phys.*, **66**, 5054 (1977).
(24) S. G. Lias, In "Kinetics of Ion Molecule Reactions", P. Ausloos, Ed., Plenum Publishing, New York and London, 1979, pp 246–249, Appendix.
(25) C. L. Currie and D. A. Ramsay, *J. Chem. Phys.*, **45**, 488 (1966).
(26) G. Maier, H. P. Reisenauer, B. Rohde, and K. Dehnicke, *Chem. Ber.*, **166**, 732 (1983).
(27) O. Kikuchi, *Chem. Phys. Lett.*, **72**, 487 (1980).
(28) (a) G. Levin and W. A. Goddard III, *J. Am. Chem. Soc.*, **97**, 1649 (1975); (b) A. F. Voter and W. A. Goddard III, *Chem. Phys.*, **57**, 253 (1981).
(29) G. Herzberg, "Molecular Spectra and Molecular Structure III. Electronic Spectra and Electronic Structure of Polyatomic Molecules", Van Nostrand, Princeton, NJ, 1967 p 142.

Table III. Vibrational Frequencies (cm^{-1}) of Allyl Radical[a]

			CH_2CHCH_2			
ω	symmetry	mode	exptl	calcd	calcd	calcd
1	a_1	CH stretch	3105	3412	3409	2543
2	a_1	CH stretch	3048	3327	2456	2459
3	a_1	CH stretch	3016	3318	3320	2409
4	a_1	CH_2 scis (sym)	1463	1661	1660	1351
5	a_1	CH_2 rock (sym)	1403	1370	1345	1148
6	a_1	CC stretch (sym)	1242	1093	1090	920
7	a_1	CCC	511	476	471	389
8	a_2	CH_2 umbrella (asym)		761	761	601
9	a_2	CH_2 twist (asym)		596	596	424
10	b_1	CH out-of-plane bend	985	1051	844	804
11	b_1	CH_2 umbrella (sym)	802	786	785	640
12	b_1	CH_2 twist (sym)	810	562	561	433
13	b_2	CH stretch	3104	3407	3407	2538
14	b_2	CH stretch	3016	3314	3314	2401
15	b_2	CH_2 scis (asym)	1463	1632	1628	1193
16	b_2	CH bend	1285	1556	1374	1361
17	b_2	CC stretch (asym)	1477	1204	1096	1003
18	b_2	CH_2 rock (asym)	1389	1040	947	779

[a] The experimental values for C_3H_5 are from the matrix IR spectra of ref 26. The calculated harmonic frequencies of allyl radical based on ab initio MCS-CF wave functions. These values are taken from Table III of ref 4.

Table IV. Experimental and Calculated Binding Energies (BE)[a]

transition	BE, eV	$E(v')$, eV	diff, eV	exptl splitting, cm^{-1}
	$CH_2{=}CH{-}CH_2^-$ $E(v') = 0.3380 + 0.0493(v' + 0.5)$			
(0,0)	0.362 ± 0.019	0.3626	0.0006	
7_0^1	0.411 ± 0.014	0.4119	0.0009	395
7_0^2	0.466 ± 0.010	0.4613	−0.0047	445
7_0^3	0.509 ± 0.009	0.5106	0.0016	350
7_0^4	0.558 ± 0.009	0.5599	0.0019	395
7_0^5	0.609 ± 0.009	0.6092	0.0002	410
7_0^6	0.655 ± 0.019	0.6586	0.0036	370
7_0^7	0.707 ± 0.019	0.7079	0.0009	420
7_0^8	0.757 ± 0.021	0.7572	0.0002	400
7_0^9	0.814 ± 0.021	0.8065	−0.0075	460
	$CH_2{=}CD{-}CH_2^-$ $E(v') = 0.3576 + 0.0485(v' + 0.5)$			
(0,0)	0.373 ± 0.019	0.3818	0.0088	
7_0^1	0.426 ± 0.014	0.4303	0.0043	430
7_0^2	0.474 ± 0.011	0.4788	0.0048	385
7_0^3	0.535 ± 0.009	0.5273	−0.0077	490
7_0^4	0.581 ± 0.011	0.5758	−0.0052	370
7_0^5	0.624 ± 0.014	0.6243	0.0003	345
7_0^6	0.667 ± 0.016	0.6728	0.0058	345
7_0^7	0.715 ± 0.018	0.7213	0.0063	390
7_0^8	0.764 ± 0.024	0.7698	0.0058	395
	$CD_2{=}CD{-}CD_2^-$ $E(v') = 0.3661 + 0.0446(v' + 0.5)$			
(0,0)	0.381 ± 0.025	0.3884	0.0075	
7_0^1	0.428 ± 0.017	0.4331	0.0051	380
7_0^2	0.472 ± 0.012	0.4777	0.0057	355
7_0^3	0.529 ± 0.009	0.5223	−0.0067	460
7_0^4	0.571 ± 0.011	0.5670	−0.0040	340
7_0^5	0.613 ± 0.016	0.6116	−0.0014	340
7_0^6	0.643 ± 0.016	0.6562	0.0132	240

[a] BE = 2.540 − CM kinetic energy. See Table I for CM KE.

CH_2CDCH_2 = 430 ± 165 cm^{-1}; (0,1) CD_2CDCD_2 = 380 ± 225 cm^{-1}. The comparison of these values with the calculated frequencies in Table III is uneven. The observed fundamentals are lower than any calculated modes but are close enough to be within the proper range for ω_7. Certainly our fitted frequencies (Table IV) match these intervals reasonably well and the observed fundamentals (Table IV) are acceptably close. Nevertheless, the large error bars accompanying the observed fundamentals (on the order of ±150 cm^{-1}) indicate that this assignment should be taken cautiously. In addition, comparison to the matrix-perturbed IR spectra strongly favors the ω_7 identity because it is the only mode observed below 800 cm^{-1}. Certainly no other modes tabulated in Table III fit our spectra nearly as well as ω_7.

C. Ion Structure. What is the structure of allyl carbanion? Direct evidence on this matter is quite sparse. An ICR study of $CH_2CHCD_2^-$ suggests that the ion is symmetric.[10] This result follows from a study of the ion chemistry of the labeled anion, $CH_2CHCD_2^-$.

$$CH_2{=}CH{-}CD_2{-}Si(CH_3)_3 + F^- \rightarrow F{-}Si(CH_3)_3 + CH_2CHCD_2^- \quad (9)$$

It is known that carbanions will react with organic nitrites.[30]

(30) G. K. King, M. M. Maricq, V. M. Bierbaum, and C. H. DePuy, *J. Am. Chem. Soc.*, **103**, 7133 (1981).

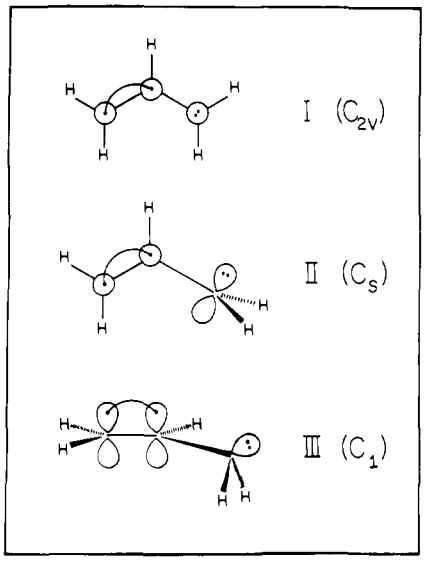

Figure 7. Three different models for the geometry of the $CH_2CHCH_2^-$ ion.

When this deuterated ion was condensed with CH_3—ONO, a 1:1 mixture of product ions was detected.

$$CH_2CHCD_2^- + CH_3—ONO \rightarrow$$
$$[CH_2CHCD_2NO{\cdot}CH_3O^-] \rightarrow CH_2CHCD{=}N—O^- + CH_3OD$$
$$[CD_2CHCH_2NO{\cdot}CH_3O^-] \rightarrow CD_2CHCH{=}N—O^- + CH_3OH \quad (10)$$

This experiment implies that $CH_2CHCH_2^-$ is a symmetric anion.

Several computational studies of the allylic ion have been reported. Two restricted Hartree–Fock (RHF) calculations report[31,32] a planar, C_{2v} structure for the negative ion and a C–C–C bond angle of roughly 133°. One minimal basis RHF calculation suggests[33] that the $CH_2CHCH_2^-$ is a nonplanar molecule; it reports a pyramidal structure for the ion with the terminal hydrogens bent out of the molecular plane by approximately 10^0. There is a general feeling that accurate calculations on weakly bound negative ions are quite difficult.[34] We should consider several possible ionic structures as we interpret the photoelectron spectra of $CH_2CHCH_2^-$.

Three qualitatively different structures for the carbanion come to mind; these are drawn in Figure 7. The first structure is the familiar C_{2v} ion (I). The second is a C_s structure with one methylene group twisted 90° out of the molecular plane (II). The last structure is a pyramidal carbanion with C_1 (or no) symmetry (III). The label of the $\tilde{X}$ $CH_2CHCH_2^-$ state is $^1A_1$ in any case. The C_{2v} ion is a fully conjugated species (I) while the C_s and C_1 structures have the ionic center uncoupled from or only partially conjugated to the CH=CH_2 group. One conjectures that the EA of a species such as II or (particularly) III would be quite small; for comparison[35] the EA(CH_3) is known to be 0.080 eV. Detachment of I might be expected to show active CCC skeletal modes in the resultant CH_2CHCH_2, ω_6 and ω_7. If other carbanion structures such as II or III were important, one might expect the vibronic signature to include twisting modes (ω_9 or ω_{12}) and rocking modes (ω_5 and ω_{18}) as active vibrations.

We are inclined to favor structure I as that describing allyl carbanion. This is suggested by two features of the spectra in Figures 3–5: (a) the simplicity of the Franck–Condon profile (only one active mode) and (b) the active vibration is an a_1 mode, ω_7. The structural differences between allyl radical and structure I (Figure 7) are small; one expects the C–C bond lengths and the CCC angle of carbanion I to be greater than the corresponding dimensions of CH_2CHCH_2. Structures II and III are qualitatively different than allyl radical; neither exhibits C_{2v} symmetry. Detachment of II or III might be expected to excite numerous skeletal modes and methylene vibrations.

The spectra in Figures 3–5 are dominated by a long progression in ω_7, the C–C–C bending mode. Each of the peaks in the photoelectron spectra is proportional to a Franck–Condon factor, FCF. Franck–Condon factors are dominated by the overlap of the vibrational wave function of the ion (Θ_i) with that of the neutral radical (Θ_r): FCF = $\langle\Theta_r|\Theta_i\rangle^2$. As we have argued earlier, no transitions in Figures 3–5 originate from vibrationally excited ions; consequently $|\Theta_i\rangle = |0\rangle$. Thus active vibrational modes in the radical ($\langle\Theta_r|$) must belong to the totally symmetric representation of a common point group encompassing both the ion and radical. This implies that if structure I of Figure 7 describes $CH_2CHCH_2^-$, the active modes in the photoelectron spectra will be confined to the a_1 block of CH_2CHCH_2 (see Table III). On the other hand, if structure II represents the allylic ion, vibrational activity is allowed in both the a_1 and b_1 blocks since both are totally symmetric under C_s. If $CH_2CHCH_2^-$ has the nonsymmetric structure III, excitation of all 18 modes of allyl radical is allowed. We have identified the sole active vibration in our photoelectron spectra as ω_7, and a_1 mode. The lack of vibronic activity in nonsymmetric modes (a_2, b_1, and b_2) suggests to us that the $CH_2CHCH_2^-$ has C_{2v} symmetry. Our qualitative picture of $CH_2CHCH_2^-$ is given by I in Figure 7; the major difference between allyl radical and the allylic ion is the enlarged C–C–C bond angle in the anion.

In an attempt to quantify the geometry change between the allyl radical and the corresponding negative ion, we have undertaken the modeling of the Franck–Condon factors for $CH_2CHCH_2^-$, $CH_2CDCH_2^-$, and $CD_2CDCD_2^-$. Our first task is to fit the experimental spectra in Figures 3–5 to a set of Gaussian peaks. The intensity of a peak centered at an energy E_k (see Table I) is fitted to a form:

$$I_k(E) = A_k \exp[-(E - E_k)^2/B_k] \quad (11)$$

The parameter A_k is a height and B_k is a width, typically 40 to 60 meV. The entire photoelectron spectrum is synthesized by simply summing these Gaussians. Using this method, we have generated excellent fits to the data. The fitted, empirical spectra for $CH_2CHCH_2^-$, $CH_2CDCH_2^-$, and $CD_2CDCD_2^-$ are presented in Figure 8 and match the experimental data (Figures 3–5) very closely. From these fitted spectra we are able to extract the areas (and thus the Franck–Condon factors (FCF)) of the peaks from the relation

$$\text{FCF} = A(\pi B)^{1/2}/2 \quad (12)$$

The Franck–Condon factors are scaled such that the top peak (C) has an area of 1.0. The final experimental FCF's are presented in Table V.

We would like to use our experimental FCF's from our fitted spectra (Figure 8, Table V) to extract an ion geometry for the allyl anion. In order to do this, we must calculate $|\Theta_i\rangle$ and $|\Theta_r\rangle$, the vibrational wave functions for the ion and neutral. The appropriate dimension is the in-plane skeletal bend of allyl. The Schrödinger equation then is

$$[2^{-1}\hbar g_{\phi\phi}{}^3\, \partial^2/\partial\rho^2 + V(\rho)]|\Theta(\rho)) = E|\Theta(\rho)) \quad (13)$$

where $V(\rho)$ is the potential energy for the bending motion of a molecule of the type Y–X–Y. In light of our observation of a harmonic spectrum for allyl, we have used $V(\rho) = [K_{vib}/2](\rho - \rho_0)^2$ where ρ is the supplement to the Y–X–Y bond angle and $\rho - \rho_0$ is the displacement from the equilibrium Y–X–Y angle in radians. The kinetic energy term contains the G-matrix element $g_{\phi\phi}{}^3$. The G element[36] is

$$g_{\phi\phi}{}^3 = r_3^{-2}\{[m_x + m_y(1 + \cos\rho_0)]/m_x m_y\} \quad (14)$$

(31) A. Pross, D. J. DeFrees, B. A. Levi, S. K. Pollack, L. Radom, and W. J. Hehre, *J. Org. Chem.*, **46**, 1693 (1981).
(32) A. C. Hopkinson and M. H. Lien, *Int. J. Quantum Chem.*, **18**, 1371 (1980).
(33) D. W. Boerth and A. Streitwieser, *J. Am. Chem. Soc.*, **100**, 750 (1978).
(34) L. Radom, In "Methods of Electronic Structure Theory", Vol. 4, H. F. Schaefer, III, Ed., Plenum Press, New York, 1977, p 333.
(35) G. B. Ellison, P. C. Engelking, and W. C. Lineberger, *J. Am. Chem. Soc.*, **100**, 2556 (1978).
(36) T. Barrow, R. N. Dixon, and G. Duxbury, *Mol. Phys.*, **27**, 1217 (1974).

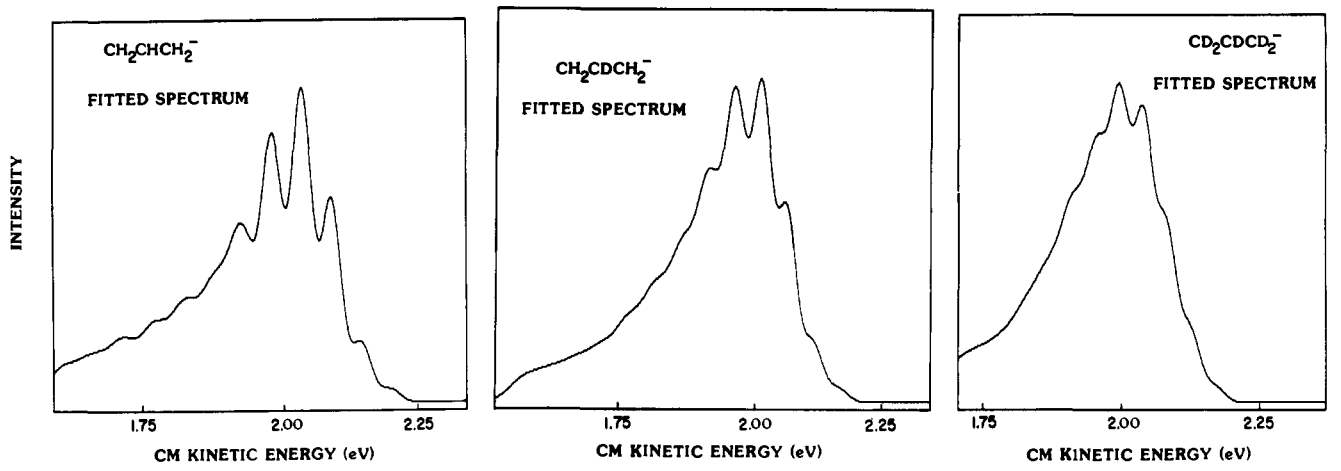

Figure 8. Fitted photoelectron spectra resulting from a Gaussian synthesis using eq 11.

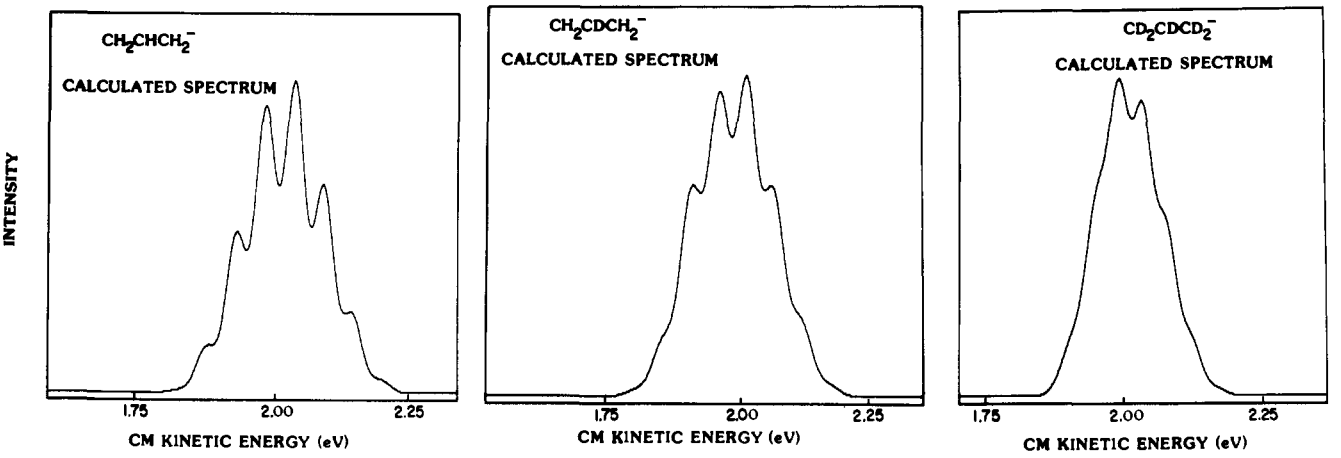

Figure 9. Calculated photoelectron spectra resulting from modeled Franck–Condon factors originating from eq 13.

The Y–X bond length is r_0. We have ignored off-diagonal elements in both the kinetic energy matrix (**G**) and the force constant matrix (**F**). In doing this we make the approximation that ω_7 is a pure bend without any contribution from stretching motion.

Using the Hamiltonian described above, we solve for the wave function $|\Theta\rangle$ variationally using a basis set of cubic B splines.[37,38] Fifty splines were sufficient for our calculations. As a check for the validity of this technique, we have applied it to the SO_2 molecule. The Franck–Condon factors for the bending motion in the $\tilde{a}\ ^3B_1 \leftarrow \tilde{X}\ ^1A_1$ electronic transition in SO_2 has been measured previously.[39] Using the experimental values for the bending frequency and the bond angle in these two states, we have calculated FCF's in excellent agreement with those found empirically. It is known[39] that SO_2 has a ground-state bond angle of 119.5° and an excited-state bond angle of 126.1 ± 0.1°. Assuming the correct ground-state geometry for SO_2, our best match to the experimental Franck–Condon factors yields an excited-state bond angle of 125.7°. The calculated FCF's are quite insensitive to the force constant K_{vib} but very sensitive to bending coordinate.

The fact that calculated FCF's are relatively insensitive to bending force constant is important in modeling the geometry of the allylic ion because the bending frequency of the anion has never been measured. The method described above was applied to the transition $CH_2CHCH_2^- \rightarrow CH_2CHCH_2$ (and appropriate deuterated isomers). We use as our equilibrium geometry for the neutral molecule the calculated parameters of Takada and Dupuis.[4] Because we only observe excitation in the bend, we believe there is little change in the geometry for the anion except in the bond angle; thus for the anion we use the C–C bond length of the neutral. We approximate allyl as having the structure Y–X–Y with Y being CH_2 (or CD_2) and X being CH (or CD). Using

Table V. Photoelectron Franck–Condon Factors[a]

transition	exptl FCF	calcd FCF
	$CH_2{=}CH{-}CH_2^-$	
(0,0)	0.045	0.043
7_0^1	0.19	0.252
7_0^2	0.64	0.665
7_0^3	1.000	1.000
7_0^4	0.82	0.854
7_0^5	0.59	0.447
7_0^6	0.41	0.128
7_0^7	0.34	0.010
7_0^8	0.27	0.002
	$CH_2{=}CD{-}CH_2^-$	
(0,0)	0.045	0.037
7_0^1	0.19	0.233
7_0^2	0.58	0.641
7_0^3	1.000	1.000
7_0^4	0.93	0.945
7_0^5	0.68	0.648
7_0^6	0.52	0.175
	$CD_2{=}CD{-}CD_2^-$	
(0,0)	0.065	0.036
7_0^1	0.23	0.223
7_0^2	0.59	0.612
7_0^3	0.96	0.981
7_0^4	1.000	1.000
7_0^5	0.82	0.658
7_0^6	0.67	0.265

[a] The uncertainty in the experimental FCF values is ±30%.

(37) C. DeBoor, *J. Approx. Theory*, **6**, 50 (1962).
(38) B. W. Shore, *J. Chem. Phys.*, **59**, 6450 (1973).
(39) J. P. Vikesland and S. J. Strickler, *J. Chem. Phys.*, **60**, 660 (1974).

Takada and Dupuis' r(C–C) = 1.388 Å and r(C–H) = 1.075 Å, we calculate effective X–Y bond lengths (r_0) of 1.505 Å (CH_2CHCH_2), 1.555 Å (CH_2CDCH_2), and 1.612 Å (CD_2CDCD_2). The vibrational frequencies in the neutral molecules are the experimental values from this experiment. The frequencies for the anions were varied along with the X–Y–X angle to obtain the best fit to our fitted FCF's.

Our best fit to the experimental FCF's was for a bond angle change of 16° with a bending frequency in the anion ($CH_2CHCH_2^-$) of about 500 cm^{-1}. The optimal fit is insensitive to the ion frequency; the bond angle changes by one degree or less across a large range of frequencies. The calculated results for the three isomers are reported in Table V. We conclude that the bond angle change between allyl anion and allyl is 16 ± 4°. We feel an uncertainty of 4° is generous even considering that we have assumed a harmonic oscillator and ignored the bond strength contribution to the bend. If one uses the calculated C–C–C angle for CH_2CHCH_2 from Takada and Dupuis of 124°, then the C–C–C angle is 140 ± 4° for $CH_2CHCH_2^-$. Note that this is not a unique answer because a bond angle decrease of 16° works equally well. We believe that the angle increases, however, because the detached electron is from an orbital which is antibonding between the terminal carbons.[33] An increasing angle is consistent with previous calculations.[31-33,40,41]

Synthesized spectra based on our calculated FCF's for the three isotopes are presented in Figure 9. One immediately notices that we have fit the data (Figures 3–5) quite well in all three cases for the first four or five peaks. For the higher vibrational states this simple model does not fit the data well at all. Note that this is also the spectral region where the peak widths seem to become larger. It is clear that something unexpected is happening in these higher levels. We do not know what this effect is, but we remind the reader that all the peaks in the absorption spectrum of allyl[25] were broadened by predissociation. This phenomenon warrants further study.

Conclusion

The allyl anion ($CH_2CHCH_2^-$) and two isotopically substituted species ($CH_2CDCH_2^-$ and $CD_2CDCD_2^-$) have been studied in negative ion photoelectron spectroscopy. The electron affinities of these three radicals as well as the heat of formation of the allyl anion ($CH_2CHCH_2^-$) are collected in Table II. The values are in fairly good agreement with previous gas-phase ion chemistry studies.[6-8]

The photoelectron spectra we observe show excitation in only one vibronic mode to be important. We identify this mode as the in-plane skeletal bend of the allyl radical. The vibrational frequencies are reported in Table III. We conclude that the major geometry change occurring when an electron is added to ground-state allyl radical is an opening in the C–C–C bond angle. A Franck–Condon analysis of our experimental peak intensities is performed. We find this bond angle to increase by about 16°.

Acknowledgment. We would like to acknowledge stimulating conversations with Larry Harding, Tony Rappe, Wes Borden, and Veronica Bierbaum. This work was supported by the United States Department of Energy (Contract DE-AC02-80ER10722).

(40) S. D. Peyerimhoff and R. J. Buenker, *J. Chem. Phys.*, **51**, 2528 (1969).
(41) S. D. Peyerimhoff and R. J. Buenker, *Theor. Chim. Acta*, **24**, 132 (1972).

Resonance Raman Studies of O_2 Stretching Vibrations in Oxygen Adducts of Cobalt Porphyrins. The Importance of Vibrational Coupling

Krzysztof Bajdor, James R. Kincaid,* and Kazuo Nakamoto*

Contribution from the Todd Wehr Chemistry Building, Marquette University, Milwaukee, Wisconsin 53233. *Received November 17, 1983*

Abstract: Studies are undertaken to examine the role of vibrational coupling in determining the $\nu(O_2)$ frequencies of molecular oxygen adducts of cobalt porphyrin complexes with a number of axial ligands. Specifically, we have carried out strategic isotopic labeling in order to demonstrate that multiple bands and shifts of $\nu(O_2)$ may arise from vibrational coupling and thus to distinguish this effect from other, steric or environmental, factors that may give rise to such behavior. Strong evidence is presented for vibrational coupling between $\nu(O_2)$ and internal modes of axial ligands that occur at comparable frequencies. The utility of mixed-isotope (^{16}O–^{18}O) experiments for detecting vibrational coupling is explored. Results, using a limited number of axial ligands (pyridine and imidazole and various substituted analogues) and several different cobalt porphyrins (tetraphenylporphine, octaethylporphine, protoporphyrin IX and diformyl deuteroporphyrin IX dimethyl esters, and picket-fence porphyrin), indicate that axial and (relatively weak) equatorial electronic effects on $\nu(O_2)$ are consistent with stabilization of charge separation in the $Co^{\delta+}$–$O_2^{\delta-}$ formulation. Also, relatively large effects on the $\nu(O_2)$ frequency are brought about by interactions of bound O_2 with solvent molecules (e.g., methylene chloride and methanol).

Introduction

The nature of dioxygen binding to myoglobin and hemoglobin has been an intensively investigated subject[1-3] during the past decade, and many model systems that reversibly bind molecular oxygen have been developed in an effort to understand the steric and electronic factors which control oxygen binding in the native proteins. These model systems include the "picket-fence",[4,5] "chelated",[6] "capped",[7,8] "strapped",[9] and "basket-handle"[10] me-

(1) Valentine, J. S. *Chem. Rev.* **1973**, *73*, 235.
(2) Wayland, B. B.; Minkiewiez, J. V.; Abd-Elmazeed, M. E. *J. Am. Chem. Soc.* **1974**, *96*, 2795.
(3) Jones, R. D.; Summerville, D. A.; Basolo, F. *Chem. Rev.* **1979**, *79*, 139.
(4) Collman, J. P.; Gagne, R. R.; Reed, C. A.; Halbert, T. R.; Lang, G.; Robinson, W. T. *J. Am. Chem. Soc.* **1975**, *97*, 1427.
(5) Collman, J. P.; Halbert, T. R.; Suslick, K. S. In "Metal Ions in Biology"; Spiro, T. G., Ed.; John Wiley: New York, 1980; Vol. 2, p 1.

0002-7863/84/1506-7741$01.50/0